Russian Geology and Geophysics © 2020, V.S. Sobolev IGM, Siberian Branch of the RAS
Vol. 61, No. 2, pp. 196–213, 2020 *DOI:10.15372/RGG2019105* *Geologiya i Geofizika*

The Nature of Low Salinity and Composition Peculiarities of Thermal Waters in Jiangxi Province (China)

S.L. Shvartsev[a,b,†], E.V. Zippa[a,b,✉], S.V. Borzenko[c]

[a] *National Research Tomsk Polytechnic University, pr. Lenina 30, Tomsk, 634050, Russia*

[b] *Tomsk Division of Trofimuk Institute of Petroleum Geology and Geophysics, Siberian Branch of the Russian Academy of Sciences, Akademicheskii pr. 4, Tomsk, 634055, Russia*

[c] *Institute of Natural Resources, Ecology and Cryology, ul. Nedorezova 16a, Chita, 672002, Russia*

Received 30 September 2018; received in revised form 25 February 2019; accepted 21 March 2019

Abstract—The chemical and isotope compositions of nitric and carbon dioxide thermal waters in Jiangxi Province (China) are considered. The nitric thermal waters are ultrafresh (TDS = 0.26–0.42 g/L) and highly alkaline (pH = 8.73–8.87), with excess of SiO_2, F^-, Na^+, etc. but ultralow concentrations of Ca^{2+}, Mg^{2+}, and Cl^-. The carbon dioxide thermal waters are more saline (TDS = 0.3–3.9 g/L) but have lower pH values (6.7–7.8). Major anions in both types of waters are HCO_3^- and Na^+, but SO_4^{2-}, F^-, CO_2, and H_2S also play a crucial role. The equilibria of the thermal waters with a complex of secondary minerals (carbonate, fluoride, clay, zeolite, etc.) have been calculated. The thermal-water–rock system is shown to be in the equilibrium–nonequilibrium state. During the transfer into deep horizons and back to the surface, the hydrotherms continuously dissolve all minerals that are in nonequilibrium with them (K-feldspar, anorthite, etc.) and form new minerals, which are in equilibrium with these waters (calcite, albite, etc.). The composition of the solution and the type of secondary minerals change with time because of the change in the proportion of chemical elements: Some elements are removed from the solution, while others continue to accumulate. A dynamic equilibrium between the elements entering and leaving the nitric thermal waters is established very early, when the waters are still ultrafresh, which is due to the high pH and low p_{CO_2}. This equilibrium inhibits an increase in the salinity of the nitric hydrotherms, and they remain lowly mineralized. Owing to the higher p_{CO_2} and, correspondingly, lower pH values, the carbon dioxide thermal waters reach a dynamic equilibrium at a later stage, when their salinity is higher than 3 g/L; therefore, they are more mineralized.

Keywords: thermal waters, chemical composition, isotope composition, equilibrium with minerals of host rocks, equilibrium–nonequilibrium system, water–rock interaction, evolution of the water–rock system, origin, composition formation

INTRODUCTION

In recent years, thermal waters have attracted special attention of scientists. This is primarily due to their wide spread in many world regions and their increasing use (Ellis and Mahon, 1977; Giggenbach, 1988; Michard, 1990; Kiryukhin et al., 2010). Of particular interest are the ultralow salinity and, at the same time, high pH values of nitric thermal waters as compared with carbon dioxide ones, which are higher mineralized but more acidic (Helvachi, 2004; Seelig and Bucher, 2010; Pasvanoğlu, 2013; Plyusnin et al., 2013; Alcicek et al., 2016; Suda et al., 2017). According to the thermal-water temperature estimated with various geochemical thermometers, the waters rise to the surface from depths of 3–4 km, but they have extremely low salinity: 0.2–0.6 g/L (nitric thermal waters) and 0.5–3.0 g/L (carbon dioxide thermal waters) (Shvartsev et al., 2018). The cause of this phenomenon must be sought in the type of thermal-water–host-rock interaction and in the equilibrium of the waters with major minerals. The saturation of waters with respect to minerals has been studied by many scientists (Arnorsson et al., 1983; Henley, 1984; Giggenbach, 1988; Grasby et al., 2000; Shvartsev et al., 2015), but there is still no explanation of the low salinity of nitric thermal waters. This problem is discussed only in our paper (Shvartsev et al., 2018).

Jiangxi Province in southeastern China is rich in carbon dioxide and nitric thermal waters, which are widely used by the residents (Li, 1979; Zhou, 1996; Sun and Li, 2001). Ninety-six thermal springs of different chemical and gas compositions were revealed within the province. They are confined to rocks and tectonic structures of different types. In this respect, the thermal waters of the study region are of great scientific interest. Therefore, a Chinese–Russian scientific expedition was organized in 2015–2017 to study the thermal waters of Jiangxi Province. It was supported by

† Deceased.
✉ Corresponding author.
E-mail address: zev-92@mail.ru (E.V. Zippa)

grants from the Russian Foundation for Basic Research, the National Natural Science Foundation of China, and, later (in 2017), the Russian Science Foundation. The results of the joint research are reported in this paper.

STUDY AREA DESCRIPTION

The climate of Jiangxi Province is humid subtropical, with a large amount of precipitation (1200–1900 mm/year). The average annual temperature is about 18.8 °C. Most of precipitation falls on May–September, and the least portion, on October–March (Jiangxi…, 2015).

Jiangxi Province is of diverse geomorphology; it has mostly mountainous and hilly topography. Mountains make up 36% of the entire territory; hills, 42%; and plains with small hills, 22%. The height of the mountains is generally less than 1000 m above sea level, seldom reaching 2200 m. The topography slopes from south to north, toward Lake Poyang located in the province zone with the lowest elevation, 30–50 m above sea level (Jiangxi…, 2015).

Jiangxi Province lies within two major tectonic structures: Yangtze Paraplatform (northern area of the province) and South China Fold System (central and southern areas of the province). The areas of both structures underwent tectonic activity and are composed of metamorphic rocks of different ages, from Proterozoic to recent. The Yangtze Paraplatform formed at 1700–2970 Ma, and the South China Fold System, at 443–542 Ma. Mesozoic and late Paleozoic rocks prevail in the study region. These are limestones, shales, dolomites, conglomerates, marls, and tuffites, which are abundant mostly in the south of the province. There are also carbonaceous strata, in particular, carbonaceous shales. In contrast to the Paleozoic rocks, the Mesozoic ones are ubiquitous and are mostly Jurassic red-colored sandstones, siltstones, mudstones, conglomerates, and limestones. The Upper Triassic strata have interbeds of carbonaceous mudstones and coals, and the Lower Cretaceous deposits have basalt and tuff interbeds, which is evident of regional tectonic activity and volcanism at that time. Jurassic granites are major intrusive rocks of the province, being most widespread in its south.

The geologic activity in Jiangxi Province in the Mesozoic led to the formation of multilevel complex structures cut by numerous faults (deep, large, and ordinary ones). Thermal waters are confined mainly to deep faults resulted from volcanic and magmatic activity and affecting the location of the thermal springs and their temperature regime. Such faults are large, reaching several hundred kilometers in strike. Basic and ultrabasic rocks are also localized along faults and influence seriously the regional geology (Zhou, 1996).

The studied springs are confined to deep faults in different geologic structures. The springs of nitric thermal waters occur predominantly within Jurassic and seldom within late Proterozoic monzonite granites, early Caledonian granites (Є–O), and Paleozoic granitoids (C–D). The granites and granitoids are composed mostly of K-feldspar (mainly microcline), plagioclase (mainly albite), quartz, and biotite (Jiangxi..., 1984).

Carbon dioxide thermal waters are discharged mostly in igneous rocks, namely, Jurassic and early Caledonian (Є-O) granites and late Proterozoic miarolites. The granites are composed mainly of K-feldspar (microcline), plagioclase (albite), quartz, and biotite. In addition, the carbon dioxide thermal springs are confined to conglomerates, sandstones, and siltstones of Cretaceous, Jurassic, Cambrian, and late Proterozoic ages. The geographical coordinates of the thermal waters, their temperature, and the geologic conditions are given in Table 1 (Jiangxi..., 1984).

METHODS AND OBJECTS

The research is based on the results of hydrogeochemical sampling made in 2015 and 2017. Eighteen samples of thermal waters (eight nitric and ten carbon dioxide thermal springs) were taken during the expeditionary research. Earlier, 11 springs (four nitric and seven carbon dioxide springs) were investigated (Sun et al., 2010). The general ion, trace-element, and isotope compositions and sulfur species were studied (Fig. 1, Table 1). The rapidly changing parameters of the waters (pH, temperature, and electrical conductivity) were determined in situ, using an AMTAST AMT03 (USA) device. Chemical analysis of the waters was carried out by several methods: HCO_3^-, CO_3^{2-}, and Cl^- were determined by titration, using an Anion 7-51 fluid analyzer; Ca^{2+} and Mg^{2+}, by AAS; F^-, SO_4^{2-}, Na^+, and K^+, by ion exchange chromatography, using an ICS-1000 Dionex chromatograph; and CO_2 was measured by titrimetry. The content of Si was determined by ICP MS, a modern high-sensitivity method, using a NexION 300D (Perkin Elmer, USA) mass spectrometer. Analysis of the isotope composition of water (D, ^{18}O) was carried out on a Finnigan MAT 253 (Thermo Scientific, USA) isotope mass spectrometer with a TC/EA-IRMS element analyzer.

Analyses were carried out in certified laboratories: the Laboratory for Hydrogeochemistry of the Water Research and Educational Center of National Research Tomsk Polytechnic University and the laboratory of the Chemical Analysis and Physical Testing Center of the East China University of Technology (Nanchang, China).

THE CHEMICAL COMPOSITION OF NITRIC THERMAL WATERS

The chemical composition of nitric thermal waters in Jiangxi Province is given in Table 2. It is seen that the waters have extremely low concentrations of chemical elements, TDS < 0.5 g/L. It is common for nitric thermal waters, because they always have low mineralization if they are not mixed with sea or other saline waters (Baskov and Surikov, 1989; Gemici and Feliz, 2001; Chudaev, 2003; Gallois, 2007; Mottl et al., 2011; Ármannsson, 2016).

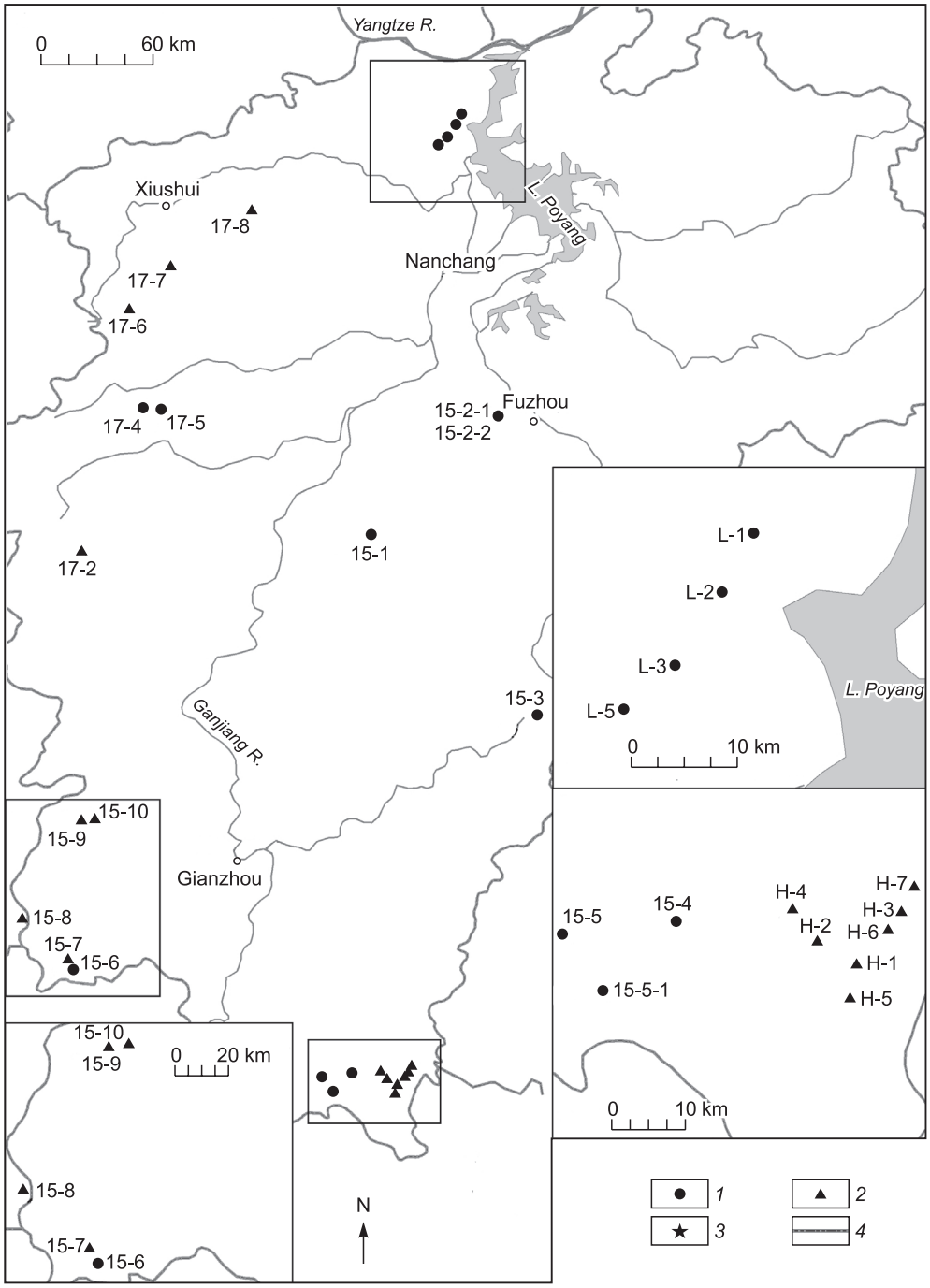

Fig. 1. Thermal waters of Jiangxi Province. *1*, carbon dioxide, *2*, nitric; *3*, capital of the province; *4*, province border. Numerals mark samples.

According to the classification by S.A. Shchukarev, the nitric thermal waters belong to either bicarbonate sodium (HCO_3–Na) or bicarbonate–sulfate sodium (HCO_3–SO_4–Na) type. The HCO_3–Na waters are characterized by TDS = 0.26–0.42 g/L (average is 0.36 g/L), and the HCO_3–SO_4–Na waters, by TDS = 0.28–0.38 g/L (average is 0.34 g/L), i.e., these waters are of nearly the same salinity. Bicarbonate sodium and bicarbonate–sulfate sodium waters also have close average pH values, 8.73 and 8.87, respectively. The salinity of both waters increases mostly at the expense of carbonate and, less, sulfate anions (Fig. 2*a*). However, its increase is accompanied by a decrease in their pH values (Fig. 2*b*) (Sun et al., 2016, 2017; Shvartsev et al., 2018).

What is the reason for this unusual phenomenon? There are two opposite trends of pH formation in nitric thermal waters. Taking into account that the studied waters occur in

Table 1. Geologic conditions of the thermal water occurrences, geographic coordinates, and temperatures of springs

Sample	Region	Coordinates		*H*, m	*T*, °C	Geologic conditions	
		N	E			Age	Rocks
Nitric thermal waters							
15-7	Neiliang (township)	114.05	25.24	369	41	J	Granites
15-8	Reshui (township)	113.54	25.32	341	38	J	Granites
15-9	Zhuangmu (township)	114.12	26.05	311	83	J	Granites
15-10	Zhuangmu (township)	114.19	26.07	276	82	J	Granites
L-1	Fujia (township)	115.92	29.42	200	71	PR_1	Tuffstones
L-2	Fujia (township)	115.92	29.41	202	65	PR_1	Tuffstones
L-3	Fujia (township)	115.92	29.41	200	65	PR_1	Tuffstones
L-5	Fujia (township)	115.92	29.41	205	69	PR_1	Tuffstones
17-2	Qianshan (city)	114.12	27.36	219	27	PR_1	Tuffstones
17-6	Wenquan (town)	114.35	28.54	233	54	J	Granites
17-7	Quqiao (town)	114.55	28.74	264	55	PR_1	Tuffstones
17-8	Tansi (township)	114.94	29.02	315	59	J	Granites
Carbon dioxide thermal waters							
15-1	Cong Ren District	115.53	27.44	75	36	K-P	Sandstones, gypsum dissemination
15-2-1	Wenguan (village)	116.13	28.00	62	41	PR_1	Tuffstones
15-2-2	Wenguan (village)	116.13	28.00	62	53	PR_1	Tuffstones
15-3	Shizui (village)	116.33	26.56	186	58	PR_1	Sandstones
15-4	Changjiang (village)	115.41	24.50	228	55	J	Granites
15-5	Zhonghe (town)	115.34	24.51	310	72	J	Granites
15-5-1	Zhonghe (town)	115.34	24.51	310	71	J	Granites
15-6	Hedong (township)	114.08	25.21	290	43	O	Limestones, marls
H-1	Nanqiaozhen (village)	115.67	24.82	450	25	J_1	Sandstones
H-2	Nanqiaozhen (village)	115.60	24.80	446	48	J_1	Sandstones
H-3	Nanqiaozhen (village)	115.70	24.83	458	37	J_1	Sandstones
H-4	Nanqiaozhen (village)	115.57	24.84	450	73	PR_1	Tuffstones
H-5	Nanqiaozhen (village)	115.64	24.73	449	27	K_2	Red-colored sandstones
H-6	Nanqiaozhen (village)	115.69	24.83	450	48	J_1	Sandstones
H-7	Nanqiaozhen (village)	115.70	24.83	430	44	J_1	Sandstones
17-4	Mabu (town)	114.42	28.06	92	29	PR_1	Tuffstones
17-5	Tianxin (town)	114.50	28.05	108	32	PR_1	Tuffstones

granite rocks composed of feldspars, plagioclases, etc., the hydrolysis of aluminosilicates is one of the processes determining the acid–base state of the water. Its typical reaction is

$$2NaAlSi_3O_8 + 11H_2O = Al_2Si_2O_5(OH)_4 + 2Na^+ + 2OH^- + 4H_4SiO_4. \quad (1)$$

The reaction proceeds with the formation of OH^-, which is usually neutralized by acids, primarily in its reaction with CO_2 (Shvartsev and Wang, 2006):

$$CO_2 + OH^- = HCO_3^-. \quad (2)$$

Under other equal conditions, a p_{CO_2} decrease leads to an increase in the pH value of the solution. The pH value also increases with the concentrations of cations in the solution (in our case, Na^+). Usually, an increase in the salinity of natural waters is accompanied by an increase in pH (Shvartsev, 1998).

However, there is also the process caused by the influence of SO_4^{2-} in nitric thermal waters. Ion SO_4^{2-} is produced through the oxidation of iron sulfide by the reaction

$$FeS_2 + 3.5O_2 + H_2O = Fe^{2+} + 2SO_4^{2-} + 2H^+. \quad (3)$$

As a result, the pH of the solution decreases, and the concentration of sulfates increases. Therefore, the relationship between pH and TDS in thermal waters is often complex (Plyusnin et al., 2013), because it depends on the proportion of acids and alkalies in the solution, which changes with time.

The temperature of the thermal waters is another factor affecting strongly the salinity. The obtained data show that the salinity of nitric thermal waters increases with temperature (Fig. 3*a*), whereas their pH decreases (Fig. 3*b*). The

Table 2. Chemical composition (mg/L) and other parameters of nitric thermal waters in Jiangxi Province

Group	Sample	pH	TDS*	CO_3^{2-}	HCO_3^-	SO_4^{2-}	Cl^-	Na^+	Ca^{2+}	Mg^{2+}	K^+	SiO_2	F^-	p_{CO_2}, $*10^{-3}$ atm	H_2S	Chemical type
I	17-2	9.05	259	10.8	114	19	4.6	62	6.3	0.04	0.88	35	6.1	0.38	2.16	HCO_3–Na
	17-8	8.97	269	30.0	87	23	4.9	73	6.0	0.005	2.76	32	10.8	0.05	27.63	HCO_3–Na
	15-7	8.70	324	12.2	127	17	6.2	72	3.8	0.02	1.98	68	15.6	0.45	0.03	HCO_3–Na
	15-9	8.50	376	6.9	131	18	4.3	76	4.2	0.05	5.09	116	14.6	0.07	0.071	HCO_3–Na
	L-5	8.61	377	8.0	174	13	5.0	89	2.1	0.15	1.70	70	14.0	0.12	–	HCO_3–Na
	L-2	8.78	407	11.0	174	13	5.1	96	2.7	0.69	2.67	90	15.0	0.10	–	HCO_3–Na
	L-3	8.62	408	8.3	186	11	5.4	110	1.9	0.1	1.56	70	15.0	0.15	–	HCO_3–Na
	L-1	8.60	421	8.6	186	14	5.5	110	1.7	0.1	2.13	80	15.0	0.11	–	HCO_3–Na
Average		8.73	355	12.0	147	16	5.1	86	3.6	0.14	2.35	70	13.3	0.18	7.47	–
II	17-7	9.02	276	14.4	53	55	1.5	55	5.1	0.05	2.68	86	2.8	0.03	4.22	HCO_3–SO_4–Na
	15-10	9.25	356	30.5	67	56	6	90	2.4	0.03	3.06	110	14.6	0.07	0.103	HCO_3–SO_4–Na
	17-6	8.72	369	3.6	77	104	6.7	83	8.1	0.047	2.74	78	5.7	0.09	0.93	HCO_3–SO_4–Na
	15-8	8.5	375	18.3	94	44	3.9	59	6.4	0.14	4.49	134	10.3	0.05	0.011	HCO_3–SO_4–Na
Average		8.87	344	16.7	73	65	4.5	72	5.5	0.07	3.24	102	8.4	0.06	1.32	–
Average for nitric thermal waters		8.80	350	14.3	110	40	4.8	79	4.5	0.11	2.79	86	10.8	0.12	4.39	HCO_3–Na

*TDS, total dissolved solids.

temperature of the thermal waters depends on the circulation depth, which, in turn, determines the time of their interaction with rocks. The deeper is waters penetrate, the longer they interact with rocks. This leads to a water salinity increase in the equilibrium–nonequilibrium state of the water–rock system (Shvartsev et al., 2015). At the same time, waters of deeper aquifers have higher concentrations of CO_2, which leads to a decrease in their pH (Fig. 3*b*). The surface temperature of hot springs is usually lower than their maximum temperature at depth (Fournier, 1991; Mutlu, 1998; Dulanya et al., 2010).

Another specific feature of the studied thermal waters is the unusual proportion of cations, with a strong predominance of Na^+ and extremely low concentrations of Ca^{2+}, Mg^{2+}, and K^+. There is an unusual relationship between the concentrations of these elements and the water TDS. For example, the total concentration of Ca^{2+} and Mg^{2+} in the nitric thermal waters decreases with an increase in not only TDS

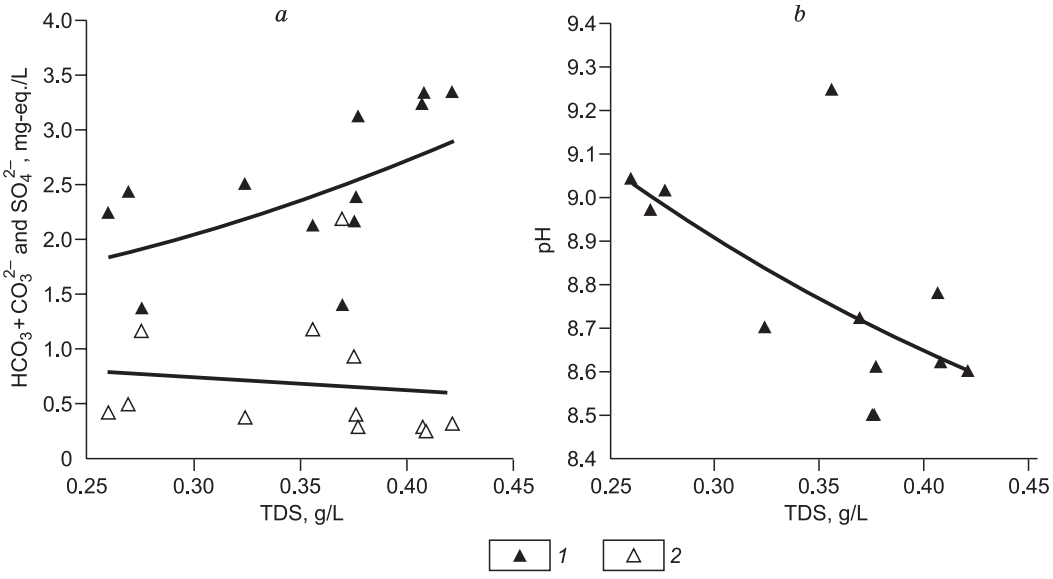

Fig. 2. Dependence of the salinity of nitric thermal waters on the concentrations of carbonate and sulfate ions (*a*) and pH (*b*). *1*, carbonate ions; *2*, sulfate ions.

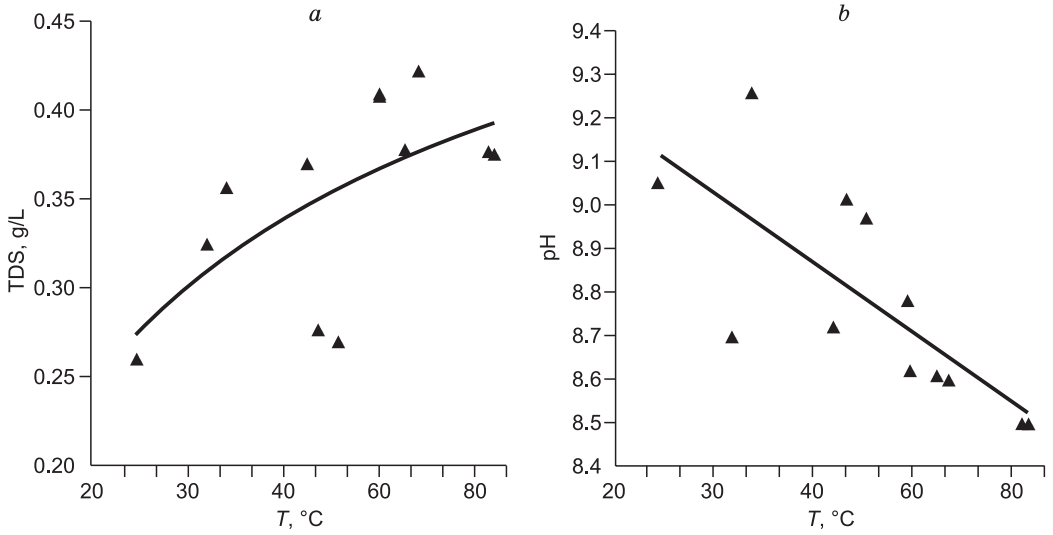

Fig. 3. Temperature dependence of the salinity (*a*) and pH (*b*) of nitric thermal waters.

(Fig. 4*a*) but also the total concentration of carbonate ions (Fig. 4*b*). All this indirectly indicates an equilibrium of nitric thermal waters with carbonate minerals: calcite, magnesite, and dolomite. During their formation, these minerals bind Ca^{2+} and Mg^{2+}, thus decreasing their concentrations with a temperature increase as a result of the decreased carbonate solubility (Fig. 4).

In contrast to Ca^{2+} and Mg^{2+}, the concentrations of SiO_2 and F^- in the studied thermal waters are high. The average concentration of F^- is 2.2 times higher than that of Ca^{2+} and 102 times higher than that of Mg^{2+}, and the concentration of SiO_2 is 19.1 and 782 times higher, respectively (Table 2). The highest concentrations of F^- are typical of HCO_3–Na thermal waters (the average is 13.3 mg/L) and, to a lesser extent, HCO_3–SO_4–Na ones (the average is 8.4 mg/L). The concentrations of SiO_2 are, on the contrary, higher in the HCO_3–SO_4–Na waters and average 102 mg/L, and in the HCO_3–Na waters they average 70 mg/L. The concentration of F^- in the nitric thermal waters increases with the concentration of carbonate ions (Fig. 5*a*) and with temperature (except for two points) (Fig. 5*b*). At the same time, there is an inverse dependence of the F^- concentration on the Ca^{2+} concentration and pH (Fig. 6). The same dependences were earlier noted by Abe (1986).

High concentrations of F^- and Si in nitric thermal waters are a well-known fact. The concentration of F^- in nitric thermal waters is usually 10–50 mg/L (Zamana, 2000; Seelig and Bucher, 2010; Deng et al., 2011; Plyusnin et al., 2013; Krunić et al., 2013; Kaasalainen et al., 2015), but sometimes it exceeds 100 mg/L (Baskov and Surikov, 1989), reaching 145 mg/L in the thermal waters of Japan (Kokubu, 1988). The concentration of SiO_2 usually ranges from 30 to

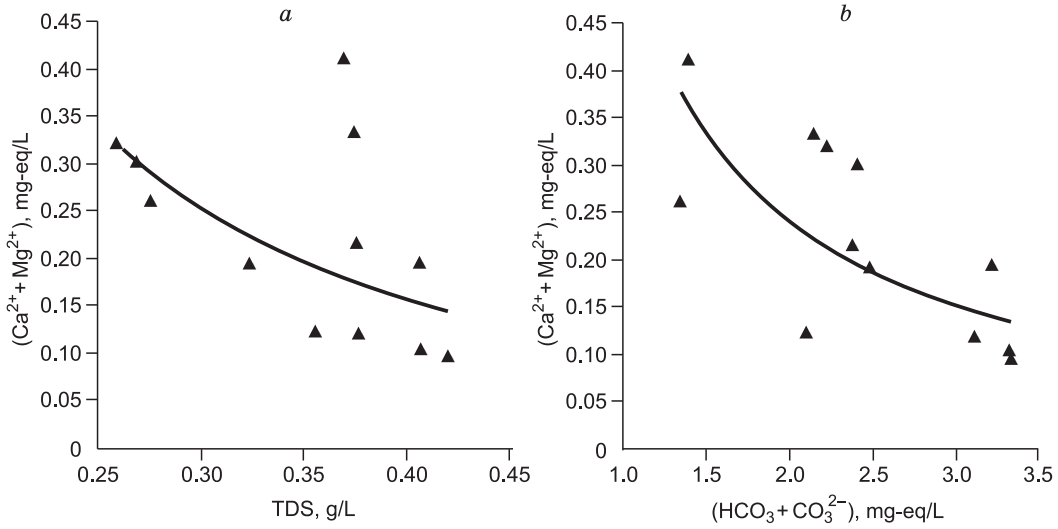

Fig. 4. Dependence of the total concentration of Ca^{2+} + Mg^{2+} in nitric thermal waters on their salinity (*a*) and the total concentration of carbonate ions (*b*).

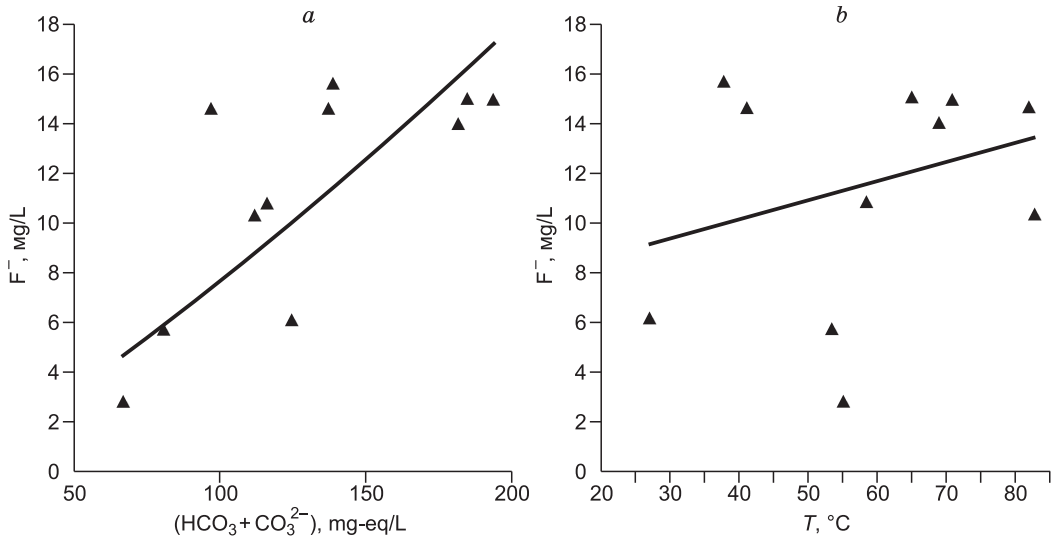

Fig. 5. Dependence of the concentration of F^- on the total concentration of carbonate ions in nitric thermal waters (*a*) and on the water temperature (*b*).

150 mg/L (Kononov, 1983; Pasvanoğlu, 2013; Alcicek et al., 2016) but sometimes reaches 500–700 mg/L. For example, the crater waters of the Mutnovsky geothermal system (Kamchatka) with a temperature of 96.1 ºC and pH = 8.3 contain 775 mg/L SiO_2 (Chudaev, 2003).

Approximately 70% of the studied nitric thermal waters contain hydrogen sulfide, but its concentration is low, <1 mg/L (except for three points). The highest concentration of H_2S, 27.63 mg/L, was found at point 17-8.

THE CHEMICAL COMPOSITION OF CARBON DIOXIDE THERMAL WATERS

The studied carbon dioxide thermal waters differ considerably in composition from the nitric ones. They are more saline, more acidic, contain CO_2, and are richer in almost all chemical components, except for SiO_2 and F^- (Table 3). Their salinity ranges from 0.3 to 3.9 g/L, averaging 1.4 g/L, and their pH varies from 6.7 to 7.8, averaging 7.0. A predominant anion is HCO_3^-, except for sample 15-3 with prevailing SO_4^{2-}. The HCO_3–Na type of waters is predominant, and the HCO_3–Na–Ca and HCO_3–SO_4–Na ones are subordinate (Sun et al., 2016, 2017; Shvartsev et al., 2018).

The studied thermal waters are dominated by HCO_3–Na and HCO_3–Na–Ca ones (group I) amounting to 52.9%. It is remarkable that these hydrotherms include both the freshest waters with TDS = 0.30–0.52 g/L (the average is 0.4 g/L; group I^a) and the most saline ones with TDS = 2.7–3.9 g/L (the average is 3.3 g/L; group I^b) (Table 3). The HCO_3–Ca

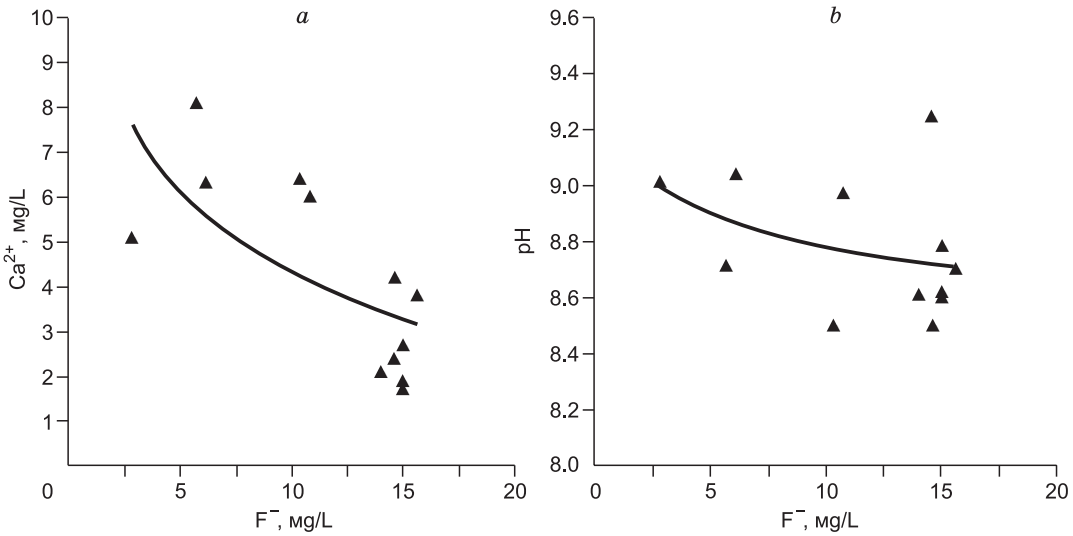

Fig. 6. Dependence of the concentration of F^- on the concentration of Ca^{2+} (*a*) and pH (*b*) of nitric thermal waters of Jiangxi Province.

Table 3. Chemical composition (mg/L) and other parameters of carbon dioxide thermal waters in Jiangxi Province

Group	Sample	*T*, °C	pH	TDS*	HCO_3^-	SO_4^{2-}	Cl^-	Na^+	Ca^{2+}	Mg^{2+}	K^+	SiO_2	F^-	p_{CO_2}, * 10^{-3} atm	H_2S	Chemical type
	H-4	73	7.30	299	106	17	8.5	72	9.9	0.09	3.1	81	1.6	1.2	–	HCO_3–Na
	15-5-1	71	7.50	351	146	23	6.4	70	12.4	0.05	2.7	77	11.7	19.4	–	HCO_3–Na
I[a]	15-5	72	7.53	364	146	26	7.1	71	12.2	0.07	3.7	83	14.3	1.0	0.009	HCO_3–Na
	H-3	37	6.74	459	217	27	8.5	94	29.1	0.09	4.4	78	1.7	54.5	–	HCO_3–Na–Ca
	15-6	43	6.86	521	250	25	5.0	91	24.5	0.5	8.3	107	9.4	34.1	0.037	HCO_3–Na
Average		59	7.19	399	173	24	7.1	80	17.6	0.16	4.4	85	7.7	22.0	0.023	
	H-6	48	6.77	2770	1428	300	35.1	711	107.8	6.74	43.2	135	3.2	150.4	–	HCO_3–Na
I[b]	15-4	55	6.78	3129	1820	257	35.5	703	90	6.1	59.2	151	7.2	123.6	0.012	HCO_3–Na
	H-1	25	6.52	3331	1886	325	81.2	699	138.5	15.37	84.6	99	2.9	1379.4	–	HCO_3–Na
	H-5	27	6.50	3869	2253	350	50.7	970	106.9	10.42	82	43	3.6	1460.3	–	HCO_3–Na
Average		39	6.64	3275	1847	308	50.6	771	110.8	9.66	67.3	107	4.2	778.4	0.012	
	15-2-1	41	6.91	287	127	38	2.7	9	51	3.0	6.0	45	4.7	18.0	–	HCO_3–Ca
II	17-4	29	7.39	356	229	27	2.0	4	64.9	10.9	0.78	18	0.5	27.0	0.11	HCO_3–Ca
	17-5	32	7.35	450	320	6	3.4	2	89	13.1	0.56	16	0.1	33.5	0.35	HCO_3–Ca
	15-1	36	6.3	1263	744	43	10.8	132	130	15.5	102.2	80	4.9	373.1	–	HCO_3–Ca–Na
Average		35	6.99	589	355	28	4.7	37	83.7	10.63	27	40	2.6	112.9	0.23	
	H-2	48	6.67	2815	1004	765	70.2	679	117.1	10.95	71.8	94	2.9	125.0	–	HCO_3–SO_4–Na
III	H-7	44	6.63	718	277	115	28.7	154	52.3	0.33	6.8	82	1.9	52.5	–	HCO_3–SO_4–Na–Ca
	15-2-2	53	7.64	346	140	50	2.1	12	61.8	2.89	15.2	57	4.6	2.5	0.383	HCO_3–SO_4–Ca
	15-3	58	7.77	987	98	465	16.9	221	39	0.15	19.5	118	9.6	0.8	0.014	SO_4–Na–Ca
Average		51	7.18	1217	380	349	29.5	267	67.6	3.58	28.3	88	4.8	45.2	0.199	–
Average for carbon dioxide thermal waters		46	7.00	1370	689	177	23.0	288	69.9	6.01	31.9	80	4.8	239.6	0.116	–

(group II) and HCO_3–SO_4–Na (group III) thermal waters are intermediate in abundance (Shvartsev et al., 2018).

A chemical analysis of the carbon dioxide thermal waters of all groups showed that the partial pressure of CO_2 (p_{CO_2}) in the aquifer is the main factor controlling their composition and salinity. The higher is p_{CO_2}, the higher is the salinity of these hydrotherms and the lower is pH (Fig. 7).

This dependence is explained by the fact that the p_{CO_2} increase highly activates the hydrolysis of aluminosilicates by carbon dioxide waters, which increases their salinity. At

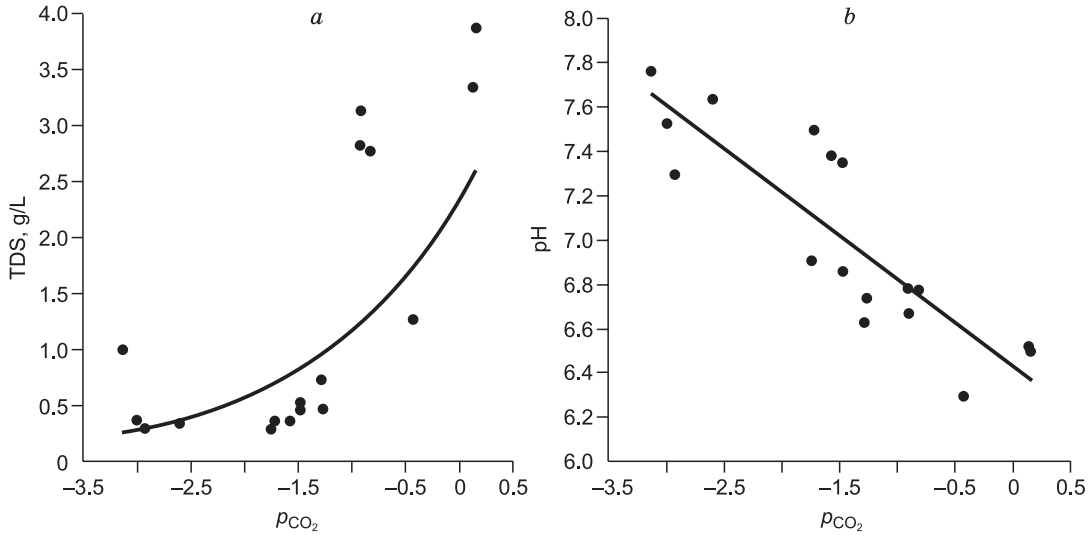

Fig. 7. Dependence of the salinity (*a*) and pH (*b*) of carbon dioxide thermal waters on the partial pressure of CO_2.

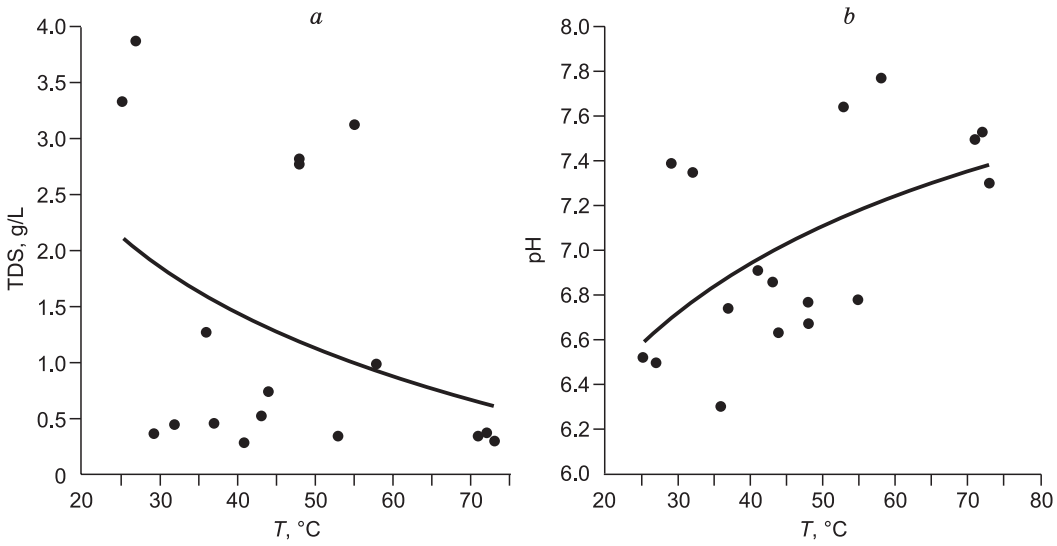

Fig. 8. Temperature dependence of the salinity (*a*) and pH (*b*) of carbon dioxide thermal waters.

the same time, OH^- interacts with CO_2 by reaction (2), which reduces pH. Low p_{CO_2} neutralizes OH^- to a lesser extent, which leads to a pH increase. Since the solubility of CO_2 decreases with a temperature increase, the hotter waters become less saline but more alkaline (Fig. 8).

The dependence of pH on the salinity of carbon dioxide thermal waters is also unusual and can be explained by the oxidation of sulfides to sulfates (Table 3, Fig. 9).

In contrast to the nitric thermal waters, the carbon dioxide waters have a minor amount of H_2S (Table 3). There is a certain relationship between the concentration of H_2S and p_{CO_2}. For example, an increase in p_{CO_2} leads to a decrease in H_2S concentration, although the carbon dioxide thermal waters contain much more SO_4^{2-} than the nitric ones (Tables 2 and 3). This is probably due to the fact that the presence of CO_2 inhibits a decrease in Eh of the thermal waters. Nevertheless, the presence of even small amounts of H_2S affects significantly the geochemical parameters of the thermal waters, including pH, which seriously complicates the relationship of some elements with their pH and salinity.

THE ISOTOPIC COMPOSITION OF THE THERMAL WATERS AND ATMOSPHERIC PRECIPITATION

To establish the genetic type of thermal waters in Jiangxi Province, we studied their isotopic composition (Table 4). A comparative analysis of the obtained data and the isotope composition of the earlier studied atmospheric precipitation (Zhou, 1996; Sun, 1998; Sun and Li, 2001) showed that all

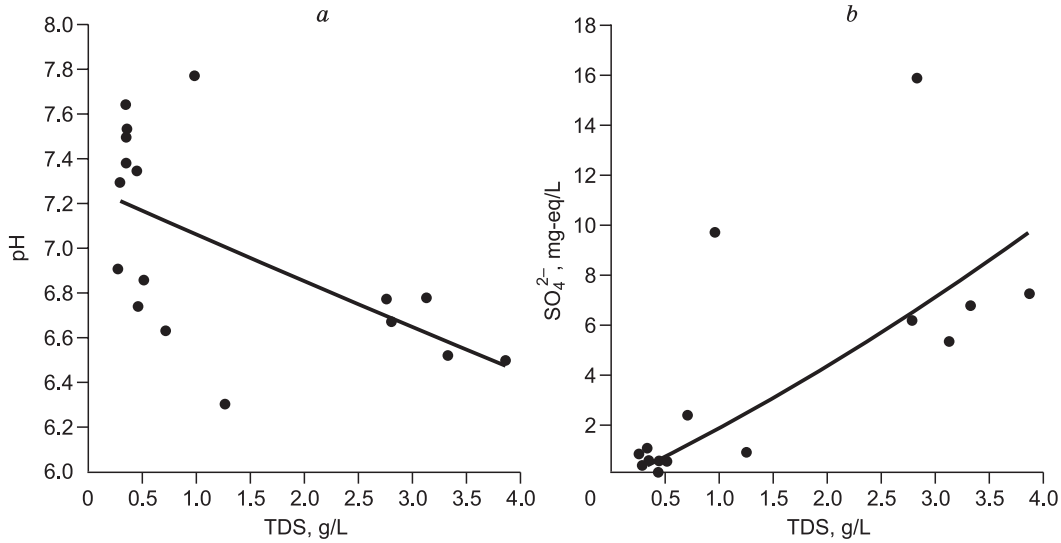

Fig. 9. Dependence of the pH (*a*) and concentrations of sulfates (*b*) of carbon dioxide thermal waters on their salinity.

Table 4. Isotopic composition of thermal waters in Jiangxi Province, ‰

Sample	δD_{vSMOW}	$\delta^{18}O_{vSMOW}$	Sample	δD_{vSMOW}	$\delta^{18}O_{vSMOW}$
Carbon dioxide thermal waters			Nitric thermal waters		
15-1	–53.1	–6.3	15-7	–57.8	–7.2
15-4	–55.9	–6.1	15-10	–66.6	–8.0
15-6	–61.0	–6.7	15-8	–59.6	–6.5
15-2-1	–47.9	–6.2	15-9	–66.2	–7.3
15-5	–60.6	–6.7	17-2	–61.8	–7.2
15-2-2	–55.0	–6.1	17-6	–59.4	–7.8
15-3	–59.0	–6.9	17-7	–53.5	–7.5
17-4	–53.1	–6.7	17-8	–62.8	–8.9

composition points of both types of thermal waters are located along the local meteoric-water line (Fig. 10). Therefore, the studied thermal waters can be referred to meteoric by origin.

At the same time, the obtained data show that the isotopic composition of all thermal waters is significantly shifted from the meteoric line toward higher $\delta^{18}O$ values. This evidences that both the carbon dioxide and the nitric thermal waters interacted for a long time with aluminosilicate minerals of endogenous rocks with high $\delta^{18}O$ values (Galimov, 1968). During this interaction, the waters continuously dissolve endogenous aluminosilicates and become enriched in ^{18}O, which results in a significant deviation of the composition points of the thermal waters from the local meteoric line. The isotope deviation is different for the nitric and carbon dioxide waters, probably, because of the different duration of their interaction with aluminosilicates, the different depths of water penetration, etc. The geochemical environment also affects the scales of ^{18}O exchange. For example, the highest concentrations of H_2S were found in samples 17-8 and 17-7 (Table 2). The isotopic-composition points of these samples lie virtually on the local meteoric-water line (Fig. 10), which is due to either the lightest oxygen isotope composition (sample 17-8) or the lightest hydrogen isotope composition (sample 17-7). The matter is that when water dissolves endogenous aluminosilicates to form clays, the latter become enriched in ^{18}O and depleted in deuterium at the expense of water. But in the presence of CO_2 in the system, water compensates the loss of ^{18}O through the isotope exchange with CO_2. Therefore, carbon dioxide thermal water remains rich in heavy oxygen isotope (Table 4). If the system is poor in CO_2 and p_{CO_2} is $<10^{-4}$ atm (Table 2), which is typical of nitric thermal waters containing H_2S, the water has a light oxygen isotope composition (Table 4). This was considered in more detail earlier (Shvartsev et al., 2017).

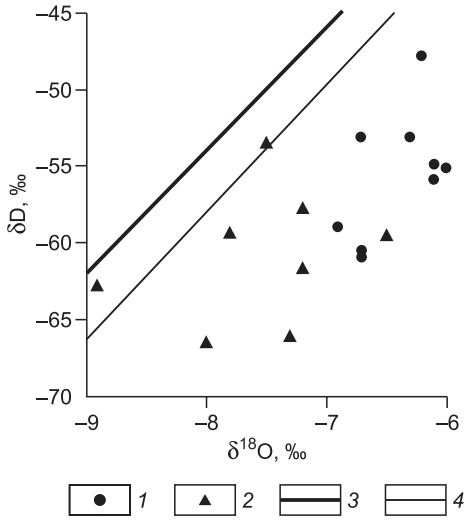

Fig. 10. δD–$\delta^{18}O$ correlation in thermal waters and atmospheric precipitation of Jiangxi Province.

THE EQUILIBRIUM OF THE THERMAL WATERS WITH MAJOR MINERALS OF WATER-BEARING ROCKS

The equilibrium of the thermal waters with primary and secondary minerals was calculated in accordance with the known methods elaborated by Garrels and Crist (1965) and using the HydroGeo software (Bukaty, 2002). The free energies of mineral formation and dissolved chemical elements were borrowed from Johnson et al. (1992). The calculations were made for 25 and 100 ºC.

The calculation showed that most of the thermal waters (nitric and carbon dioxide ones) are in equilibrium with calcite, magnesite, and fluorite despite their different TDS and pH values (Fig. 11). Since the solubility of carbonates decreases with a temperature increase, the degree of the equilibrium increases with depth. Therefore we believe that all thermal waters are in equilibrium with carbonate minerals at a certain depth. In our opinion, a local nonequilibrium is possible only during the rise of thermal waters to the surface and their cooling and dilution with groundwater.

Another mineral saturating the studied thermal waters is fluorite (Fig. 11*b*). Most of the thermal waters are in equilibrium with both fluorite and carbonates. In contrast to carbonates, the solubility of fluorite increases with temperature. Nevertheless, water–fluorite equilibrium is observed in

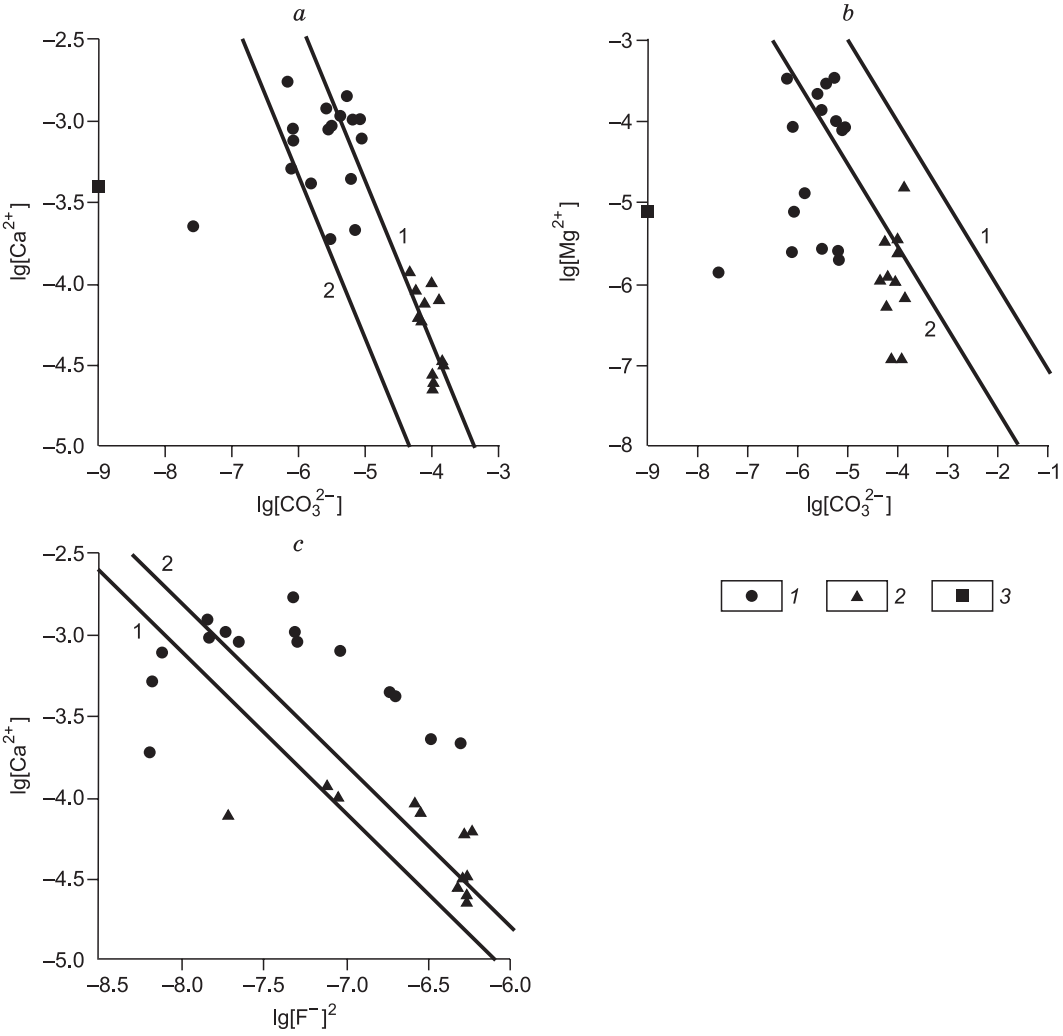

Fig. 11. Equilibrium of thermal waters with calcite (*a*), magnesite (*b*), and fluorite (*c*) at 25 °C (line 1) and 100 °C (line 2). *1*, carbon dioxide thermal waters; *2*, nitric thermal waters; *3*, atmospheric precipitation.

more than 50% of the water samples even at 100 ºC and in more than 70% at the real temperature. Rising to the surface, the thermal waters are diluted with groundwater and become saturated with fluorite (as well as calcite) even at their extremely low salinity (0.2–0.3 g/L at pH > 8.2). In contrast to hypergenesis zone waters (Shvartsev, 1998), the geochemical parameters of thermal ones with precipitated calcite and fluorite are similar, although Ca^{2+} precipitates with CO_3^{2-} in the first case and with F^- in the second.

The equilibrium of thermal waters with aluminosilicate minerals predominant in the regional host rocks is more complex (Fig. 12). The nitric and carbon dioxide thermal waters show absolutely different saturation with respect to aluminosilicate minerals. The nitric thermal waters are in equilibrium with laumontite, albite, talc, glaucophane, muscovite, and microcline, whereas the carbon dioxide waters are in equilibrium mostly with montmorillonite, less often, with illite and kaolinite (minerals that form mainly in the weathering crust), and, seldom, with laumontite, albite, muscovite, and microcline. This phenomenon is explained by the higher pH values. The nitric thermal waters have higher pH than the carbon dioxide ones, which ensures a shift of their equilibrium to the stability field of more exotic minerals (Shvartsev et al., 2015).

Figure 12 presents the calculated thermodynamic parameters of the equilibrium of the studied thermal waters with some silicates and aluminosilicate minerals. The stability fields of the main minerals, such as anorthite, labradorite, forsterite, and augite, lie significantly higher than others in the plots. It turned out that all igneous Ca-, Mg-, and Fe-aluminosilicates forming the rock (anorthite, labradorite, fayalite, forsterite, and augite), as well as enstatite, diopside, heulandite, almandine, grossular, pyrope, and gehlenite, are in permanent nonequilibrium with any hydrotherms. Thermal waters always dissolve aluminosilicates to produce secondary minerals. At the same time, the composition of such authigenic minerals does not remain constant but changes during the water–rock interaction.

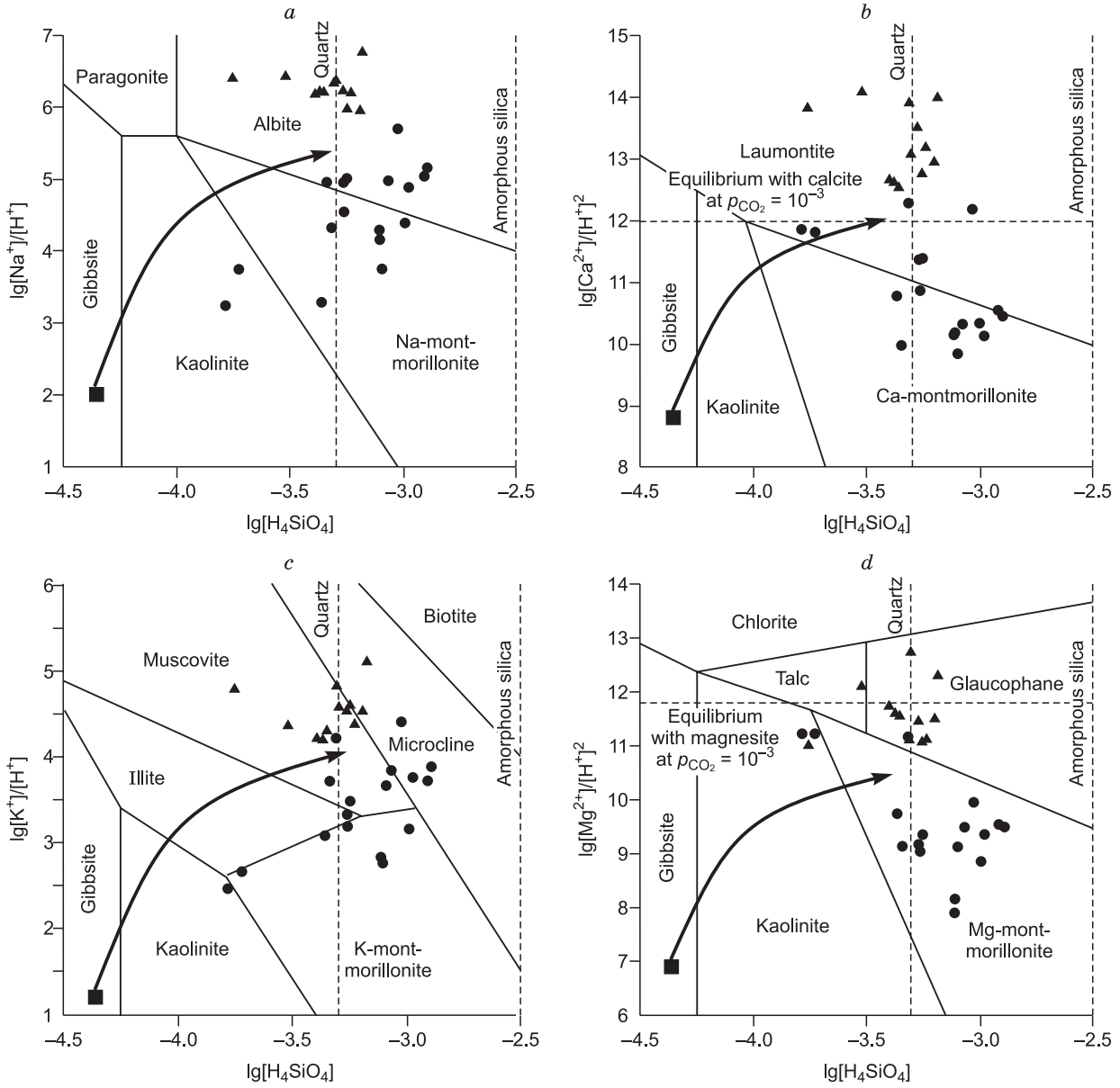

Fig. 12. Equilibrium of thermal waters with aluminosilicate minerals. *a*, In the system HCl–H_2O–Al_2O_3–Na_2O–SiO_2 at 100 °C; *b*, in the system HCl–H_2O–Al_2O_3–CaO–SiO_2 at 100 °C; *c*, in the system SiO_2–Al_2O_3–K_2O–CO_2–H_2O at 100 °C; *d*, in the system HCl–H_2O–Al_2O_3–MgO–SiO_2 at 100 °C. Designations follow Fig. 11.

As seen from Fig. 12, the first mineral that forms in rocks with atmospheric precipitation is kaolinite. The subsequent water–rock interaction results in montmorillonite, illite, and calcite, i.e., minerals typical of the hypergenesis zone. As water percolates to depth (Shvartsev et al., 2018), albite, laumontite, muscovite, microcline, biotite, glaucophane, talc, chlorite, etc. (minerals of hydrothermal genesis) appear among the secondary minerals. This assemblage of secondary minerals is specific to nitric and, much less, carbon dioxide thermal waters; the latter waters seldom reach the stage of secondary-mineral formation.

Consequently, although the nitric thermal waters have salinity 5–10 times lower than the carbon dioxide ones (Tables 2 and 3), they are significantly ahead in the composition evolution and related secondary-mineral formation. This apparent contradiction is explained by the fact that the average pH values of the nitric thermal waters are by a factor of 1.26 higher than those of the carbon dioxide waters. Therefore, the former contain almost 60 times more OH^- than the latter. Under alkaline conditions, the secondary-mineral formation accelerates, which prevents the accumulation of chemical elements in the solution and, thus, inhibits an increase in its salinity. The problem of low salinity and accompanying high pH values of the nitric thermal waters will be discussed below, and now we will return to equilibrium.

The analysis has shown an intricate equilibrium of the thermal waters with various minerals. The water is in nonequilibrium with dissolving minerals but is in equilibrium with forming ones. Shvartsev (1991, 1995, 1998) called this phenomenon an equilibrium–nonequilibrium state as early as 1978. The equilibrium–nonequilibrium state of the water–rock system is well correlated with the fact that water interacts with endogenous aluminosilicates according to the dissolution–precipitation principle developed by many famous scientists (O'Neil and Taylor, 1967; Helgeson and Murphy, 1983; Putnis, 2002; Hellmann et al., 2003; Fu et al., 2009; Zhu and Lu, 2009).

Consequently, the water–rock system is in an equilibrium–nonequilibrium state. It is contradictory and can produce new solids and liquids. The water–rock interaction is not a particular or local phenomenon limited in time but a strictly directed global continuous rock transformation by water, yielding absolutely new products. This interaction is the internal state of the water–rock system, which does not depend on external factors but is determined by the composition and structure of water, without which it cannot exist. The cessation of the interaction leads to the disappearance of the system. It is crucial that there are no natural forces that can stop this process. The internal mechanisms of the above interaction determine the continuous evolution of the water–endogenous-aluminosilicate system (Shvartsev, 2012, 2013, 2014, 2016). All this significantly changes our idea of the evolution of the surrounding world, which is a nonlinear, irreversible, and continuous process (Shvartsev, 2009, 2010, 2015), and provides a better understanding of the evolution of hydrotherm composition. The presented data on the equilibrium between the thermal waters and rock minerals confirm our concept.

THE CAUSE OF THE LOW SALINITY AND SPECIFIC COMPOSITION OF THE THERMAL WATERS

The temperature at the water circulation depth was estimated by hydrogeochemical methods, based on the concentrations of dissolved components sensitive to temperature changes during the water–rock interaction and the temperature of thermal springs. Calculation with a Si-geothermometer (Fournier, 1977) yielded the depth temperatures of nitric and carbon dioxide thermal waters from 85 to 147 ºC and from 62 to 153 ºC, respectively. Taking into account that the geothermal gradient for Jiangxi Province is 25 ºC/km (Wan, 2012) and using the formula given by Li and Li (2010), the circulation depths of nitric and carbon dioxide thermal waters are 2.8–5.3 km and 1.8–5.6, respectively.

Hence, the thermal waters percolate to a depth of 3–5 km, are heated to 150 ºC, and interact with rocks and many nonequilibrium minerals for a long time, continuously dissolving them, but remain fresh. This is especially true for the nitric thermal waters with TDS ≤ 0.4 g/L (Table 2). These waters are much less saline than most types of waters in the hypergenesis zone, which occur at a shallow depth, are cold, and have an age of several thousand years (Shvartsev, 1998). The carbon dioxide thermal waters are characterized by a higher TDS, reaching 3.9 g/L (Table 3), but this is also not high for deep waters. This phenomenon is related to the specific evolution of the water–rock system, which is considered below.

It is shown above that the interaction of thermal waters with aluminosilicate minerals continues throughout their occurrence in rocks both during their infiltration in the geologic section and during their emergence (Shvartsev et al., 2018). But the chemical elements that accumulate in the solution as a result of dissolution of endogenous minerals are continuously bound by secondary minerals: Ca^{2+}, by calcite, montmorillonite, zeolites, and other aluminosilicates; Mg^{2+}, by glaucophane, chlorite, and zeolites; Na^{+}, by albite and zeolites; K^{+}, by biotite, illite, muscovite, microcline, etc.; and F^{+}, by fluorite and, partly, micas (Figs. 11 and 12). The presence of these secondary minerals is confirmed by results of petrographic and mineralogical studies performed in the study area (Huang et al., 2002; Legros et al., 2019). Binding of the accumulated chemical elements by secondary minerals permits the system to reach both chemical and dynamic equilibria and establishes a balance between the amount of elements entering the solution and the amount of elements leaving it. Such secondary minerals are produced not simultaneously but successively, in accordance with the laws of their solubility: Poorly soluble minerals are the first to form, and readily soluble ones are the last (Shvartsev, 1994, 1995, 1998, 2010, 2012, 2014).

According to the thermodynamic laws, gibbsite is the first to form, because an aqueous solution with pH = 5 becomes saturated with this mineral by the reaction

$$Al^{3+} + 3OH^{-} = Al(OH)_3, \quad (4)$$

with its constant at 25 ºC expressed as

$$K = 1/[Al^{3+}][OH^{-}]^3 = 10^{33.2}, \quad (5)$$

when the Al^{3+} activity is equal to $10^{-6.2}$ mol/L. This activity value is reached rapidly, for time T_1 (Fig. 13). From this moment, gibbsite begins to form, which leads to a change in the proportion of Al and Si in the solution. Since the interaction of water with endogenous rocks continues and the content of Si in them is higher than that of Al, silicon, in contrast to aluminum, continues to accumulate in the solution. This finally leads to an equilibrium between the dissolved components and produced kaolinite (Shvartsev, 2010, 2012, 2014):

$$2Al^{3+} + 6OH^{-} + 2H_4SiO_4 = Al_2Si_2O_5(OH)_4 + 5H_2O, \quad (6)$$

with the constant of this reaction at 25 ºC expressed as

$$K = 1/[Al^{3+}]^2[OH^{-}]^6[H_4SiO_4]^2 = 10^{7.94}. \quad (7)$$

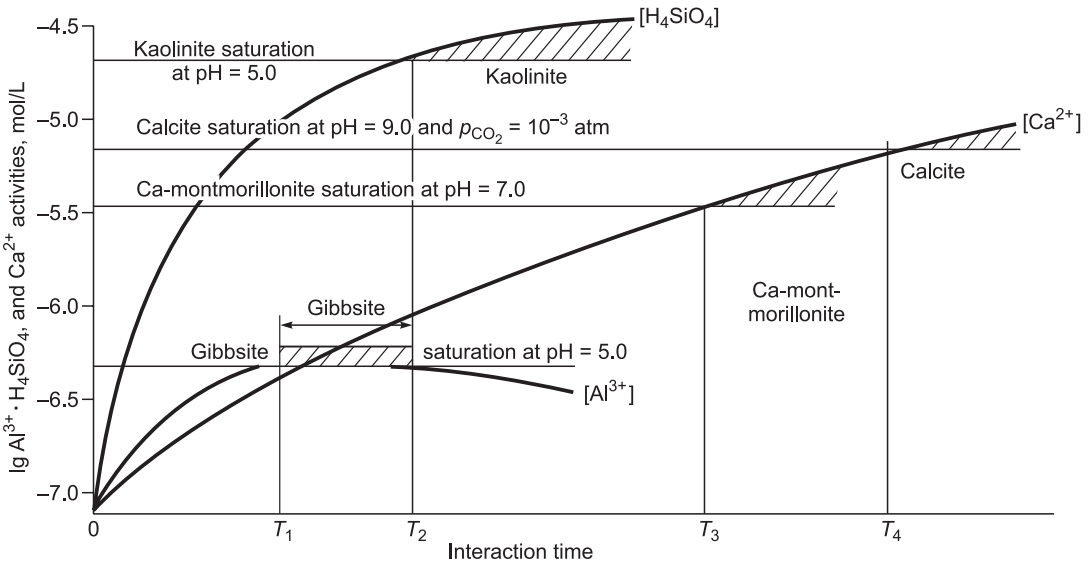

Fig. 13. Changes in the composition of secondary minerals depending on the duration of the groundwater–basalt interaction.

At pH = 5.0, this equilibrium is reached only at the activity of H_4SiO_4 equal to $10^{-4.7}$ mol/L. Kaolinite binds Si and Al in equal amounts, and the amount of Si entering the solution is 2.74 times higher than that of Al. For this reason, Si continues to accumulate in the solution, in contrast to Al, which again leads to a change in their proportion.

During the formation of kaolinite, the solution has a deficit of Al. The kaolinite formation depends on the amount of arriving Al but not Si, which is present in excess. Therefore, produced kaolinite binds almost all Al entering the solution and only part of Si, necessary for building the kaolinite crystal lattice.

Consequently, kaolinite forms later than gibbsite. It results from the longer interaction of water with endogenous minerals; we designate the interaction time as T_2 (Fig. 13). Since kaolinite binds not all dissolved Si, the latter continues to accumulate in water after the beginning of the mineral formation. In accordance with reaction constant (5), the activity of Al^{3+} cannot increase and, moreover, must decrease at a constant pH value. This disturbs the equilibrium between the water and gibbsite because of the formation of kaolinite instead of gibbsite under these conditions (Shvartsev, 2010, 2012, 2014).

The nonequilibrium state of the water–rock system even after its saturation with kaolinite ensures its subsequent evolution. The next mineral to form is Ca-montmorillonite. It is produced in the solution with higher concentrations of Ca, Si, and OH^- by the reaction

$$0.167Ca^{2+} + 2.33Al^{3+} + 3.67\ H_4SiO_4 + 7.32\ OH^- = Ca_{0.167}Al_{2.33}O_{10}(OH)_2 + 10H_2O, \quad (8)$$

with its constant at 25 ºC expressed as

$$K = 1/[Ca^{2+}]^{0.167}[Al^{3+}]^{2.33}[OH^-]^{7.32}[H_4SiO_4]^{3.67} = 10^{89.3}. \quad (9)$$

The formation of montmorillonite is a longer process than the formation of kaolinite (Fig. 13), as it requires accumulation of larger amounts of Ca^{2+}, Si, and OH^- in the solution. Therefore, this mineral is produced after gibbsite, kaolinite, and some iron minerals not considered here (Shvartsev, 2010, 2012, 2014).

Calcite forms later than montmorillonite (Fig. 13). Establishment of an equilibrium of thermal waters with carbonate and clay minerals is a more serious geochemical barrier, which inhibits the accumulation of Ca^{2+}, Mg^{2+}, Fe, K^+, and Al in the waters. Therefore, the concentrations of these elements remain low (Tables 2 and 3). Clay minerals bind only part of Si. Thus, the concentrations of Si and Na in the thermal waters continue to increase, which ensures the formation of other secondary minerals. Under these conditions, the pH of the waters continues to increase. A temperature increase with depth shifts the water–carbonate equilibrium to still lower concentrations of Ca^{2+}, Mg^{2+}, and Fe in the solution at the same pH.

The thermal waters in equilibrium with carbonate and clay minerals stay in nonequilibrium with many endogenous aluminosilicates, which continue to dissolve, thus supplying the solution with all chemical elements. Most of these elements are immediately bound by secondary minerals. Since the concentrations of some elements (Si, Na^+, F^-, etc. (Tables 2 and 3)) continue to increase, the equilibrium shifts from the kaolinite and montmorillonite fields to the above-bordering ones (Fig. 12). The waters reach an equilibrium with laumontite, epidote, glaucophane, chlorite, talc, and many other minerals (Fig. 12). These waters have low concentrations of Ca^{2+}, Mg^{2+}, and Fe (Table 2), which are controlled by the behavior of the carbonate system at high pH. Thus, the water–rock system passes to a higher hydrothermal stage of the evolution.

Until the system evolution stops, the concentrations of some chemical elements, even those that are associated with secondary minerals (Si, Na^+, F^-, and K^+), will continue to increase with time because of the different proportions of these elements in dissolved and precipitated compounds (Shvartsev, 1991). As the temperature increases at the next stage, the water becomes saturated with the main mineral phases of granitic rocks (albite, muscovite, biotite, microcline, etc.), and these minerals no longer dissolve but begin to precipitate as new mineral complexes. In addition, each mineral phase forms at the certain stage of the water–rock system evolution and is controlled by its composition and thermodynamic parameters.

Thus, during the evolution of the water–rock system, the water tends to an equilibrium with most of rock minerals that form but do not dissolve. Obviously, this system will never be completely balanced, because an equilibrium between the water and many Ca-, Mg-, and Fe-aluminosilicates of abyssal genesis (e.g., anorthite, fayalite, forsterite, diopside, titanite, etc.) can never be attained. Although granites prevail in Jiangxi Province, thermal waters reach depths of 3–5 km, where rocks of different compositions exist. It is crucial that chemical elements pass from soluble minerals into the solution that has already reached an equilibrium with many secondary minerals; therefore, these elements can precipitate to form minerals.

Thus, water interacts with rocks even at great depths, but a large portion of chemical elements entering the solution precipitates as new minerals. This permits the system to reach both chemical and dynamic equilibria and establishes a balance between the elements entering the solution and the precipitating ones. As a result, the salinity of thermal waters decreases and remains constant or slightly increases with time.

Why does the water salinity remain low? An equilibrium of thermal waters with minerals of granites and zeolites in alkaline conditions is established at the low activities of chemical elements forming secondary minerals (Huang et al., 2002; Legros et al., 2019), because the constants of the reactions of hydrolysis of these minerals are extremely low (Table 5).

At high pH and low p_{CO_2}, the above equilibrium is attained at low concentrations of Na^+, K^+, Ca^{2+}, Mg^{2+}, and Fe in the solution, i.e., at extremely low water salinity. This does not mean that the water–rock interaction stops. It continues, but almost all elements entering the solution, despite their low concentrations, immediately precipitate in the form of other minerals (Huang et al., 2002; Legros et al., 2019).

If an additional amount of ambient acid, e.g., CO_2, enters the system, then the p_{CO_2} of the solution increases, whereas the pH decreases (Fig. 7). In this case, an equilibrium is also established but at higher concentrations of prevailing elements in the solution or at its higher salinity.

Consequently, water controls the composition of precipitating secondary minerals and thus changes its own composition. This, together with additional elements supplied from dissolved minerals, favors the formation of other secondary minerals, which leads to an additional change in the solution and, hence, to the formation of new minerals. This is the main essence of the evolution of the water–rock system, which proceeds at any salinity of the solution. In the case of nitric thermal waters, the system evolves at low salinity, because it has a high pH (Huang et al., 2002; Shvartsev, 2017; Legros et al., 2019).

CONCLUSIONS

(1) The geologic and geomorphological conditions in Jiangxi Province (China) are favorable for the formation and discharge of nitric and carbon dioxide thermal waters. This is mainly due to a significant difference in the regional topography, the Mesozoic tectonic activity in the region, and abun-

Table 5. Constants of the reactions of hydrolysis (H_2O or $H_2O + CO_2$) of some aluminosilicate and silicate minerals at 100 °C

No.	Mineral	Hydrolysis reaction	Reaction constant			
			H_2O		$H_2O + CO_2$	
			lgK	lgY*	lgK	lgY*
1	Muscovite	$KAl_3Si_3O_{10}(OH)_2 + 10H_2O = K^+ + 3Al^{3+} + 3H_4SiO_4 + 10OH^-$	–120.90	–7.11	–117.40	–6.53
2	Margarite	$CaAl_4Si_2O_{10}(OH)_2 + 10H_2O = Ca^{2+} + 4Al^{3+} + 2H_4SiO_4 + 14OH^-$	–148.20	–7.06	–141.60	–6.15
3	Paragonite	$NaAl_3Si_3O_{11}H_2O + 10H_2O = Na^+ + 3Al^{3+} + 3H_4SiO_4 + 10OH^-$	–118.60	–6.98	–115.30	–6.41
4	Laumontite	$CaAlSi_3O_8 + 8H_2O = Ca^{2+} + 2Al^{3+} + 4H_4SiO_4 + 8OH^-$	–90.53	–6.30	–83.95	–4.94
5	Microcline	$KAl_3Si_3O_8 + 8H_2O = K^+ + Al^{3+} + 3H_4SiO_4 + 4OH^-$	–52.11	–5.79	–48.80	–4.07
6	Analcime	$NaAlSi_2O_6 \cdot H_2O + 5H_2O = Na^+ + Al^{3+} + 2H_4SiO_4 + 4OH^-$	–46.00	–5.75	–42.68	–4.74
7	Biotite	$KFe_3AlSi_3O_{10}(OH)_2 + 10H_2O = K^+ + 3Fe^{3+} + 3H_4SiO_4 + 10OH^-$	–102.70	–5.70	–99.33	–5.23
8	Albite	$NaAlSi_3O_8 + 8H_2O = Na^+ + Al^{3+} + 3H_4SiO_4 + 4OH^-$	–50.00	–5.55	–46.71	–4.67
9	Glaucophane	$Na_2Mg_3Al_2SiO_{22}(OH)_2 + 22H_2O = 2Na^+ + 3Mg^{2+} + 2Al^{3+} + 8H_4SiO_4 + 14OH^-$	–151.90	–5.24	–145.30	–4.69
10	Chlorite	$Mg_6Si_4O_{10}(OH)_8 + 10H_2O = 6Mg^{2+} + 4H_4SiO_4 + 12OH^-$	–101.90	–4.63	–95.29	–3.97
11	Talc	$Mg_3Si_4O_{10}(OH)_2 + 10H_2O = 3Mg^{2+} + 4H_4SiO_4 + 6OH^-$	–58.30	–4.49	–51.75	–3.45

*Conventional constant, i.e., the reaction constant taken relative to the number of the reacting components in the solution (Shvartsev et al., 2007).

dant deep but permeable faults (often, normal faults). All this favored the formation of large hydrodynamic systems with long groundwater transition zones in the region. Some of these zones contain CO_2 arriving from deeper horizons, whereas others lack it. In the first case, carbon dioxide thermal waters form, and in the second, nitric waters are spread.

(2) The regional nitric and carbon dioxide thermal waters differ significantly from each other. The nitric thermal waters are ultrafresh (TDS = 0.26–0.42 g/L; the average is 0.35 g/L), highly alkaline (pH = 8.5–9.3; the average is 8.8), with high concentrations of SiO_2, F, and other components and low ones of Ca and Mg. The carbon dioxide thermal waters are more saline (TDS = 0.29–3.87 g/L; the average is 1.37 g/L), more acidic (pH = 6.3–7.8; the average is 7.0), with average SiO_2 concentrations close to those in the nitric thermal waters, and with higher Ca and Mg and lower F concentrations.

(3) Almost all studied thermal waters are in equilibrium with carbonates (calcite and magnesite), kaolinite, montmorillonite, and illite. Most of the nitric thermal waters and part of the carbon dioxide ones are also in equilibrium with albite, muscovite, microcline, laumontite, glaucophane, talc, etc. Thus, the thermal waters and the minerals of the host rocks form a unique equilibrium–nonequilibrium system, in which water dissolves minerals that are in nonequilibrium with it but forms other secondary minerals, which are in equilibrium with it and are stable in this medium.

(4) The equilibrium–nonequilibrium water–aluminosilicate system can have a long geologic evolution: The aqueous solution continuously accumulates certain chemical elements, whereas others are bound by secondary minerals. This causes not only a serious change in the solution composition but also a change of secondary minerals by others.

(5) The low salinity of the nitric thermal waters is explained by the fact that the low concentrations of CO_2 and other acids lead to a rapid increase in pH and, hence, an equilibrium of the waters with many secondary minerals. As a result, the amount of elements bound by secondary minerals quickly becomes equal to the amount of elements entering the solution. The establishment of a dynamic equilibrium between the inflow of certain elements into the solution and the removal of others from it inhibits an increase in the salinity of the nitric thermal waters. The same balance of elements in the more acidic carbon dioxide thermal waters is reached much later. It has not been reached in the study area.

The work was financially supported by grant 15-55-53122 GFEN_a from the Russian Foundation for Basic Research, project 17-17-01158 from the Russian Science Foundation, and project 41511130031 from the National Natural Science Foundation of China.

REFERENCES

Abe, K., 1986. Fluoride ion content of the hot spring waters in the central and southern parts of the Kii peninsula, Wakayama Prefecture. Japan. Bull. Geol. Sur. Jap. 37 (9), 479–489.

Alcicek, H., Bulbul, A., Alcicek, M.C., 2016. Hydrogeochemistry of the thermal waters from the Yenice Geothermal Field (Denizli Basin, Southwestern Anatolia, Turkey). J. Volcanol. Geotherm. Res. 309, 118–138.

Ármannsson, H., 2016. The fluid geochemistry of Icelandic high temperature geothermal areas. Appl. Geochem. 66, 14–64.

Arnorsson, S., Gunnlaugsson, E., Svavarsson, H., 1983. The chemistry of geothermal waters in Iceland. II. Mineral equilibria and independent variables controlling water compositions. Geochim. Cosmochim. Acta 47, 547–566.

Baskov, E.A., Surikov, S.N., 1989. The Earth's Thermal Waters [in Russian]. Nedra, Leningrad.

Bukaty, M.B., 2002. Designing of software for the solution of hydrogeological problems. Izvestiya TPU 305 (6), 348–365.

Chudaev, O.V., 2003. Composition and Conditions of Formation of Recent Hydrothermal Systems in the Russian Far East [in Russian]. Dal'nauka, Vladivostok.

Deng, Y., Nordstrom, D.K., McCleskey, R.B., 2011. Fluoride geochemistry of thermal waters in Yellowstone National Park: I. Aqueous fluoride speciation. Geochim. Cosmochim. Acta 75 (16), 4476–4489.

Dulanya, Z., Morales-Simfors, N., Sivertun, A., 2010. Comparative study of the silica and cation geothermometry of the Malawi hot springs: Potential alternative energy source. J. Afr. Earth Sci. 57, 321–327.

Ellis, A.J., Mahon, W.A.J., 1977. Chemistry and Geothermal Systems. Academic Press, London.

Fournier, R.O., 1977. Chemical geothermometers and mixing models for geothermal systems. Geothermics 5, 41–50.

Fournier, R.O., 1991. Water geothermometers applied to geothermal energy, in: D'Amore, F., Application of Geochemistry in Geothermal Reservoir Development. United Nations Institute of Training and Research, Rome, pp. 37–69.

Fu, Q., Konishi, H., Xu, H., Seyfried, W.E., Jr., Zhu, C., 2009. Coupled alkali–feldspar dissolution and secondary mineral precipitation in batch systems: 1. New experiments at 200 °C and 300 bars. Chem. Geol. 258 (3-4), 125–135.

Galimov, E.M., 1968. Geochemistry of Stable Carbon Isotopes [in Russian]. Nedra, Moscow.

Gallois, R., 2007. The formation of the hot springs at Bath Spa, UK. Geol. Mag. 144 (4), 741–747.

Garrels, R.M., Christ, Ch.L., 1965. Solutions, Minerals and Equilibria. Harper & Row, New York.

Gemici, U., Filiz, S., 2001. Hydrochemistry of the Cesme geothermal area in western Turkey. J. Volcanol. Geotherm. Res. 110, 171–187.

Giggenbach, W.F., 1988. Geothermal solute equilibria. Derivation of Na–K–Mg–Ca geoindicators. Geochim. Cosmochim. Acta 52, 2749–2765.

Grasby, S.E., Hutcheon, I., Krouse, H.R., 2000. The influence of water–rock interaction on the chemistry of thermal springs in Western Canada. Appl. Geochem. 15 (4), 439–454.

Helgeson, H.C., Murphy, W.M., 1983. Calculation of mass transfer among minerals and aqueous solutions as a function of time and surface area in geochemical processes. I: Computational approach. Mathem. Geol. 15, 109–130.

Hellmann, R., Penisson, J.-M., Hervig, R.L., Thomassin, J.-H., Abrioux, M.-F., 2003. An EFTEM/HRTEM high-resolution study of the near surface of labradorite feldspar altered at acid pH: evidence for interfacial dissolution–reprecipitation. Phys. Chem. Mineral. 30 (4), 192–197.

Helvachi, C., 2004. Hydrogeochemical and hydrogeological integration of thermal waters in the Emet area (Kutahya, Turkey). Appl. Geochem. 1, 105–118.

Henley, R.W., Truesdell, A.H., Barton, P.B., Jr., Whitney, J.A., 1984. Reviews in Economic Geology. Vol. 1. Fluid–Mineral Equilibria in Hydrothermal Systems. Society of Economic Geologists, Littleton.

Huang, X.L., Wang, R.C., Chen, X.M., Hu, H., Liu, C.S., 2002. Vertical variations in the mineralogy of the Yichun topaz–lepidolite granite, Jiangxi Province, southern China. Can. Mineral. 40, 1047–1068.

Jiangxi Bureau of Geology and Mineral Resources, 1984. Regional Geology of Jiangxi Province: Geological Memoirs of Ministry of Geology and Mineral Resources. People's Republic of China, Beijing, Geological Publishing House, Vol. 1, No. 2.

Jiangxi Statistical Yearbook, 2015. http://www.jiangxi.gov.cn/ (accessed 01 February 2016).

Johnson, J.W., Oelkers, E.H., Helgeson, H.C., 1992. SUPCRT92: A software package for calculating the standard molal thermodynamic properties of minerals, gases, aqueous species, and reactions from 1 to 5000 bar and 0 to 1000 °C. Comput. Geosci. 18, 899–947.

Kaasalainen, H., Stefánsson, A., Giroud, N., Arnórsson, S., 2015. The geochemistry of trace elements in geothermal fluids, Iceland. Appl. Geochem. 62, 207–223.

Kiryukhin, A.V., Kiryukhin, V.A., Manukhin, Yu.F., 2010. Hydrogeology of Volcanogenic Basins [in Russian]. Nauka, St. Petersburg.

Kokubu, N., 1988. Fluorine content in natural waters. Bull. Univ. Elec. Commun. 1 (1), 173–177.

Kononov, V.I., 1983. Geochemistry of thermal waters in recent volcanism areas (rift zones and island arcs), in: Transactions of the Geological Institute of the Academy of Sciences of the USSR [in Russian]. Moscow, Vol. 379.

Krunić, O., Parlić, S., Polomčić, D., Jovanović, M., Erić, S., 2013. Origin of fluorine in mineral waters of Bujanovac valley (Serbia, Europe). Geochem. Int. 51 (3), 205–220.

Legros, H., Richard, A., Tarantola, A., Kouzmanov, K., Mercadier, J., Vennemann, T., Marignac, C., Cuney, M., Wang, R.C., Charles, N., Bailly, L., Lespinasse, M.Y., 2019. Multiple fluids involved in granite-related W–Sn deposits from the world-class Jiangxi province (China). Chem. Geol. 508, 92–115.

Li, G., Li, F., 2010. The Circulation Law, Sustainable Development and Utilization of Geothermal Water in Guanzhong Basin. Science Press, Beijing.

Li, X., 1979. The relationship between distribution of thermal waters and uranium mineralization in Jiangxi. J. East China Geol. Inst. 2, p. 21–29.

Michard, G., 1990. Behavior of major elements and some trace elements (Li, Rb, Cs, Sr, Fe, Mn, W, F) in deep hot water from granitic areas. Chem. Geol. 89, 117–134.

Mottl, M.J., Seewald, J.S., Whet, C.G., Tivey, M.K., Michael, P.J., Proskurowski, G., McCollom, T.M., Reeves, E., Sharkey, J., You, C.-F., Chan, L.-H., Pichler, T., 2011. Chemistry of hot springs along the Eastern Lau Spreading Center. Geochim. Cosmochim. Acta 75 (4), 1013–1038.

Mutlu, H., 1998. Chemical geothermometry and fluid–mineral equilibria for the Omer Gecek thermal waters, Afyon area, Turkey. J. Volcanol. Geotherm. Res. 80, 303–321.

O'Neil, J.R., Taylor, H.P., 1967. The oxygen isotope and cation exchange chemistry of feldspars. Am. Mineral. 52 (9–10), 1414–1437.

Pasvanoğlu, S., 2013. Hydrogeochemistry of thermal and mineralized waters in the Diyadin (Ağri) area, Eastern Turkey. Appl. Geochem. 38, 70–81.

Plyusnin, A.M., Zamana, L.V., Shvartsev, S.L., Tokarenko, O.G., Chernyavskii, M.K., 2013. Hydrogeochemical peculiarities of the composition of nitric thermal waters in the Baikal Rift Zone. Russian Geology and Geophysics (Geologiya i Geofizika) 54 (5), 495–508 (647–664).

Putnis, A., 2002. Mineral replacement reactions: from macroscopic observations to microscopic mechanisms. Mineral. Mag. 66, 689–708.

Seelig, U., Bucher, K., 2010. Halogens in water from the crystalline basement of the Gotthard rail base tunnel (central Alps). Geochim. Cosmochim. Acta 9, 2581–2595.

Shvartsev, S.L., 1991. Interaction of water with aluminosilicate rocks. Geologiya i Geofizika (Soviet Geology and Geophysics) 32 (12), 16–50 (13–37).

Shvartsev, S.L., 1995. The problem of self-organization of a water–rock geological system. Geologiya i Geofizika (Russian Geology and Geophysics) 36 (4), 22–29 (17–24).

Shvartsev, S.L., 1998. Hydrogeochemistry of the Hypergenesis Zone [in Russian]. Nedra, Moscow.

Shvartsev, S.L., 2009. Self-organizing abiogenic dissipative structures in the geologic history of the Earth. Earth Sci. Front. 16 (6), 257–275.

Shvartsev, S.L., 2010. Where did global evolution begin? Her. Russ. Acad. Sci. 80 (2), 173–182.

Shvartsev, S.L., 2012. The internal evolution of the water-rock geological system. Her. Russ. Acad. Sci. 82 (2), 134–142.

Shvartsev, S.L., 2013. Water as the main factor of global evolution. Her. Russ. Acad. Sci. 83 (1), 78–85.

Shvartsev, S.L., 2014. How do complexities form? Her. Russ. Acad. Sci. 84 (4), 300–309.

Shvartsev, S.L., 2015. The basic contradiction that predetermined the mechanisms and vector of global evolution. Her. Russ. Acad. Sci. 85 (4), 342–351.

Shvartsev, S.L., 2016. Unknown mechanisms of granitization of basalts. Her. Russ. Acad. Sci. 86 (6), 513–526.

Shvartsev, S.L., 2017. Evolution in nonliving matter: Nature, mechanisms, complication, and self-organization. Her. Russ. Acad. Sci. 86 (6), 513–526.

Shvartsev, S.L., Wang Yanxing, 2006. Geochemistry of sodic waters in the Datong intermountain basin, Shanxi Province, northwestern China. Geochem. Int. 44 (10), 1015–1026.

Shvartsev, S.L., Ryzhenko, B.N., Alekseev, V.A., Dutova, E.M., Kondrat'eva, I.A., Kopylova, Yu.G., Lepokurova, O.E., 2007. Geologic Evolution and Self-Organization of the Water–Rock System. Vol. 2. The Water–Rock System in Hypergenesis Zone [in Russian]. Izd. SO RAN, Novosibirsk.

Shvartsev, S.L., Zamana, L.V., Plyusnin, A.M., Tokarenko, O.G., 2015. Equilibrium of nitrogen-rich spring waters of the Baikal Rift Zone with host rock minerals as a basis for determining mechanisms of their formation. Geochem. Int. 53 (8), 713–725.

Shvartsev, S.L., Kharitonova, N.A., Lepokurova, O.E., Chelnokov, G.A., 2017. Genesis and evolution of high-pCO_2 groundwaters of the Mukhen spa (Russian Far East). Russian Geology and Geophysics (Geologiya i Geofizika) 58 (1), 37–46 (48–59).

Shvartsev, S.L., Sun, Z., Borzenko, S.V., Gao, B., Tokarenko, O.G., Zippa, E.V., 2018. Geochemistry of the thermal waters in Jiangxi Province, China. Appl. Geochem. 96, 113–130.

Suda, K., Gilbert, A., Yamada, K., Yoshida, N., Ueno, Y., 2017. Compound– and position–specific carbon isotopic signatures of abiogenic hydrocarbons from on-land serpentinite-hosted Hakuba Happo hot spring in Japan. Geochim. Cosmochim. Acta 206, 201–215.

Sun, Zh., 1998. Geothermometry and chemical equilibria of geothermal fluids from Hveragerdi, SW-Iceland, and selected hot springs Jiangxi Province, SE-China. The United Nations University Geothermal Training Program, Report 14, pp. 373–402.

Sun, Zh., Li, X., 2001. Studies of geothermal waters in Jiangxi Province using isotope techniques. Sci. China, Series E 44, 144–150.

Sun, Zh., Liu, J., Gao, B., 2010. Hydrogeochemistry and Direct Use of Hot Springs in Jiangxi Province, SE-China. Proceedings of the World Geothermal Congress, Bali, Indonesia.

Sun, Zh., Gao, B., Shvartsev, S., Tokarenko, O., Zippa, E., 2017. The Thermal Water Geochemistry in Jiangxi Province (SE-China). Procedia Earth Planet. Sci. 17, 940–943.

Sun, Zh., Shvartsev, S.L., Tokarenko, O.G., Zippa, E.V., Gao, B., 2016. Geochemical peculiarities of nitric thermal waters in Jiangxi Province (SE-China), in: IOP Conference Series: Earth and Environmen-

tal Science. All-Russian Scientific Conference with International Participation on Contemporary Issues of Hydrogeology, Engineering Geology and Hydrogeoecology in Eurasia, 23–27 November 2015, Tomsk, Russia. Vol. 33.

Wan, T.F., 2012. The tectonics of China. Higher Education Press, Beijing.

Zamana, L.V., 2000. Fluorine in nitric hydrothermal waters of Transbaikalia. Geologiya i Geofizika (Russian Geology and Geophysics) 41 (11), 1575–1581 (1520–1527).

Zhou, W., 1996. Studies of geothermal background and isotopic geochemistry of thermal water in Jiangxi Province, in: China Nuclear Science and Technology Report. China Atomic Energy Press, Beijing.

Zhu, C., Lu, P., 2009. Alkali feldspar dissolution and secondary mineral precipitation in batch systems. 3. Saturation states of product minerals and reaction paths. Geochim. Cosmochim. Acta 73 (11), 3171–3200.

Editorial responsibility: A.E. Kontorovich